RSC Advances

RSC Publishing

PAPER

View Article Online
View Journal | View Issue

Graphitic carbon quantum dots as a fluorescent sensing platform for highly efficient detection of Fe^{3+} ions†

Cite this: *RSC Advances*, 2013, **3**, 3733

Yong-Lai Zhang,[ac] Lei Wang,[c] Heng-Chao Zhang,[b] Yang Liu,[b] Hai-Yu Wang,[c] Zhen-Hui Kang*[b] and Shuit-Tong Lee*[a]

Received 19th December 2012,
Accepted 11th January 2013

DOI: 10.1039/c3ra23410j

www.rsc.org/advances

Reported here is a green synthesis of graphitic carbon quantum dots (GCQDs) as a fluorescent sensing platform for the highly sensitive and selective detection of Fe^{3+} ions. Through the electrochemical ablation of graphite electrodes in ultrapure water, uniform GCQDs with graphitic crystallinity and oxygen containing groups on their surfaces have been successfully prepared. The absence of acid, alkali, salt and organic compounds in the starting materials effectively avoids complex purification procedures and environmental contamination, leading to a green and sustainable synthesis of GCQDs. The oxygen functional groups (*e.g.*, hydroxyl, carboxyl) contribute to the water solubility and strong interaction with metal ions, which enable the GCQDs to serve as a fluorescent probe for the highly sensitive and selective detection of Fe^{3+} ions with a detection limit as low as 2 nM. The high sensitivity of our GCQDs could be attributed to the formation of complexes between Fe^{3+} ions and the phenolic hydroxyls of GCQDs. The fluorescence lifetime of GCQDs in the presence and absence of Fe^{3+} was tested by time-correlated single-photon counting (TCSPC), which confirmed a dynamic fluorescence quenching mechanism.

1 Introduction

In recent years, fluorescent carbon materials, represented by carbon quantum dots (CQDs)[1,2] and graphene quantum dots (GQDs),[3,4] have attracted enormous research interest due to their promising potential in fluorescent probes,[5] photovoltaic devices,[6] photocatalysis,[2] and bioimaging.[7] To date, despite a short history, carbon-based quantum dots have revealed a cornucopia of both novel photophysical properties and potential applications. For instance, CQDs bearing only carbon and oxygen containing groups are biocompatible, and thus they are considered as potential candidates for biochemical analysis and tissue engineering.[8] Additionally, CQDs are both electron donors and acceptors in photoexcited states, which make them promising for applications in novel optoelectronic devices.[9] Besides their strong photoluminescence in a broad spectral range, usually from the visible to near IR region, CQDs exhibit clear upconversion PL properties, which holds great promise for photocatalyst design.[2,10]

The exceptional properties of CQDs have continuously stimulated the rapid development of novel methodologies for CQD preparation. Ever since the first synthesis of CQDs by laser ablation,[1] various synthetic strategies, including ultrasonic treatment,[11] microwave synthesis,[12] electrochemical approaches,[13–15] carbon soot,[16] dehydration of carbohydrates,[17] reverse micelles,[18] and even hydrothermal treatment of natural grass[19] have been developed for CQD synthesis. However, these methods usually suffer from harsh preparative conditions, low yield and especially complex purification procedures which generally involve centrifugation, column chromatography and long dialysis times. Moreover, most of the reported CQDs prepared by using organic compounds (*e.g.*, glucose, ascorbic acid and citric acid) as a carbon source behave somewhat like macromolecules. Therefore, a green and simple approach to the mass production of CQDs with graphitic character, here called graphitic carbon quantum dots (GCQDs), is highly desired.

On the other hand, as an alternative to semiconductor quantum dots (SQDs, *e.g.*, CdS, PbSe and CdSe),[20,21] CQDs have been widely used as a fluorescent probe for the detection of metal ions.[19,22] As compared with conventional SQDs, CQDs not only avoid the environmental and health concerns arising from the toxicity of heavy metal ions, but they also exhibit biocompatibility, high sensitivity and selectivity. Despite the fact that there exist several successful examples of using CQDs or GQDs as fluorescent sensing materials for the detection of metal ions such as Cu^{2+} and Hg^{2+},[19,22,23] as well as the discrimination of Fe^{3+} and Fe^{2+} in living cells,[24] the highly

[a]*Center of Super-Diamond and Advanced Films (COSDAF) and Department of Physics and Materials Science, City University of Hong Kong, Hong Kong SAR, P. R. China. E-mail: apannale@cityu.edu.hk*

[b]*Institute of Functional Nano & Soft Materials (FUNSOM) and Jiangsu Key Laboratory for Carbon-Based Functional Materials & Devices, Soochow University, Suzhou, P. R. China. E-mail: zhkang@suda.edu.cn*

[c]*State Key Laboratory on Integrated Optoelectronics, College of Electronic Science and Engineering, Jilin University, 2699 Qianjin Street, Changchun, 130012, P. R. China*

† Electronic supplementary information (ESI) available. See DOI: 10.1039/c3ra23410j

sensitive and selective detection of metal ions on the basis of brand-new sensing mechanisms is still of great importance for the exploration of the full potential of CQD-based advanced fluorescent sensors.

In this work, we report a green and facile synthesis of GCQDs as a fluorescent sensing platform for the highly sensitive and selective detection of Fe^{3+}. Through the electrochemical ablation of graphite electrodes in the presence of only ultrapure water, GCQDs with uniform particle size have been successfully prepared without the need of complex purification procedures. The as-prepared GCQDs can serve as a fluorescent probe for the highly efficient detection of Fe^{3+} ions due to the formation of complexes between Fe^{3+} ions and the phenolic hydroxyls of GCQDs. The fluorescent quenching mechanism was also investigated with time-correlated single-photon counting (TCSPC) experiments.

2 Experimental

2.1 Preparation of GCQDs

In a typical electrochemical synthesis of GCQDs, graphite rods (99.99%, Alfa Aesar Co. Ltd.) were adopted as both anode and cathode, as well as the carbon source; ultrapure water was used as the electrolyte. After the graphite rods were inserted into the ultrapure water (300 mL) with a distance of about 6 cm, static potentials of 50 V were applied to the two electrodes through a direct current power supply. After reaction for 4 days with stirring, the transparent solution turned to a homogeneous dark-brown solution, indicating the presence of small carbon particles. Then, the obtained solution was filtered, and centrifuged at 22 000 rpm for 30 min to remove the bulky graphite fragments, and the GCQD solution was finally obtained.

2.2 Metal ion detection

For the detection of various metal ions, $FeCl_3$, $AgNO_3$, $CuCl_2$, $CaCl_2$, $Zn(NO_3)_2$, $CoCl_2$, $Hg(NO_3)_2$, $MgCl_2$, $AlCl_3$, $MnCl_2$, $PbCl_2$, $CdCl_2$, $FeCl_2$, and $NiCl_2$ have been used as various ion sources. All chemicals were used as received without further purification. GCQD solution (10 μg L^{-1}, 1 μL) was added into the solutions containing a calculated amount of ions. The PL spectra were recorded after reaction for 5 s. The excitation wavelength was fixed at 340 nm for all the PL spectra.

2.3 Characterization

Transmission electron micrographs (TEM) were taken on a FEI-Tecnai F20 (200 kV) transmission electron microscope (FEI). X-Ray photoelectron spectroscopy (XPS) was performed using an ESCALAB 250 spectrometer. Spectra were baseline corrected using the instrument software. UV-vis absorption spectra were recorded on an Agilent 8453 UV-visible spectrophotometer. Fluorescent spectrophotometry was performed using a FluoroMax 4 (Horiba Jobin Yvon) spectrophotometer. Nanosecond fluorescence lifetime experiments were performed with a time-correlated single-photon counting (TCSPC) system under right-angle sample geometry. A 379 nm picosecond diode laser (Edinburgh Instruments EPL375, repetition rate 2 MHz) was used to excite the samples. The fluorescence was collected by a photomultiplier tube (Hamamatsu H5783p) connected to a TCSPC board (Becker & Hickl SPC-130). The time constant of the instrument response function (IRF) was about 300 ps.

3 Results and discussion

It is worth pointing out that, in our experiments, the GCQDs were prepared by electrochemical ablation of graphite electrodes in the presence of only pure water, without the addition of any acid, alkali, salts or organic compounds. The absence of other chemicals directly leads to a green and sustainable strategy towards GCQD synthesis. Especially, as compared with other methods, complex purification is not necessary, and therefore, the preparation procedures are significantly simplified. Moreover, the as-prepared GCQDs are very homogeneous in particle size. Shown in Fig. 1 are TEM images of the GCQDs. It can be clearly identified from the images that the nanodots are monodisperse. The particle size distribution shows that the diameters of the GCQDs are in the range of 1–9 nm, with an average value of ~5 nm (inset of Fig. 1a). HR-TEM further confirms the particle size and the graphitic character. The lattice of the (002) plane of graphite with an interplanar spacing of 0.32 nm could be easily identified. Fig. 1b shows that the as-prepared GCQDs are all highly crystalline, which could also be confirmed from wide-angle XRD patterns (ESI†, Fig. S1). The formation of the graphitic crystallinity of these GCQDs could be attributed to the graphite electrodes, as the GCQDs could be considered as fragments of the graphite rods. Remarkably, the unique graphitic character of our GCQDs may distinguish them from amorphous CQDs prepared from the carbonization of organic compounds, and GQDs.

In order to characterize the surface chemical composition of the GCQDs, X-ray photoelectron spectroscopy (XPS) was applied to a dry GCQD sample. As shown in the survey X-ray photoelectron spectrum (Fig. 2a), only C and O signals were detected, indicating that the carbon nanoparticles possess only oxygen containing groups. The oxygen atom content is measured to be 35.5%. The C1s spectrum of the sample shows three peaks at 284.6, 286.6 and 288.5 eV, which are attributed to C–C (non-oxygenated ring carbon), C–O (hydroxyl and epoxy carbon), and C=O (carbonyl), respectively (Fig. 2b).[25] Obviously, the as-prepared GCQDs are very rich in oxygen; the content of carbon not bonded to oxygen is ~59%; and the contents of C–O and C=O are 18% and 23%, respectively. Beside the XPS spectrum, the FT-IR spectrum was also used for the identification of oxygen containing groups (Fig. S2, ESI†). Typically, the peaks around 3345 cm^{-1} could be ascribed to the stretching vibrations of –OH, whereas the peaks located around 1444 cm^{-1} and 1706 cm^{-1} indicate the existence of carbonyl (C=O). These results confirm that the GCQDs are functionalized with oxygen containing groups such as carboxyl, epoxyl and hydroxyl.

A Raman spectrum was measured to confirm the graphitic character of our GCQD sample. As shown in Fig. 3 the

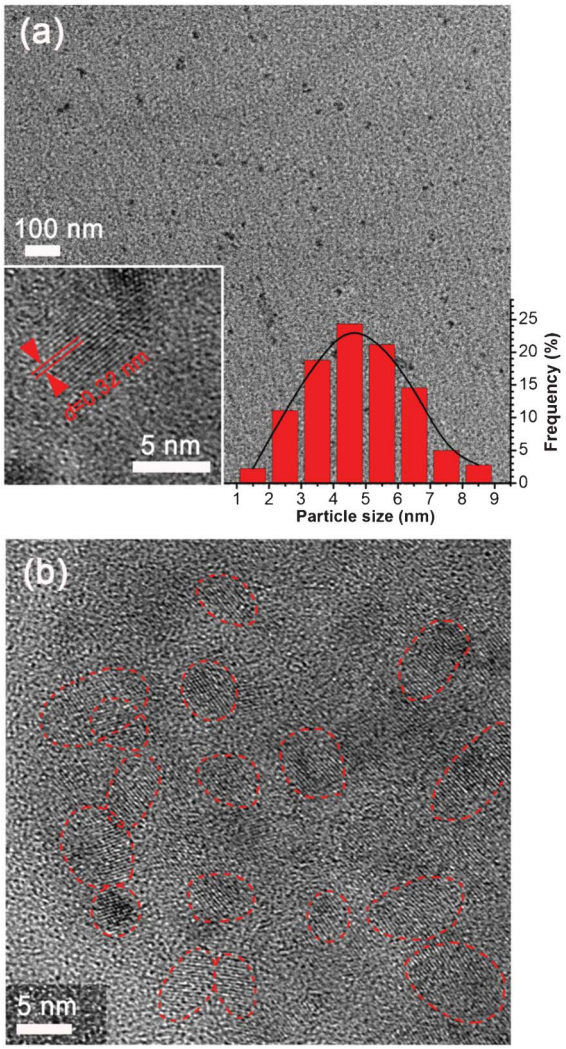

Fig. 1 (a) TEM image of the as-prepared GCQDs, the insets show a HR-TEM image of a GCQD with graphitic crystalline and the particle size distribution calculated based on 500 nanoparticles. (b) HR-TEM image of the as-prepared GCQDs. The red lines indicate the edges of different nanoparticles.

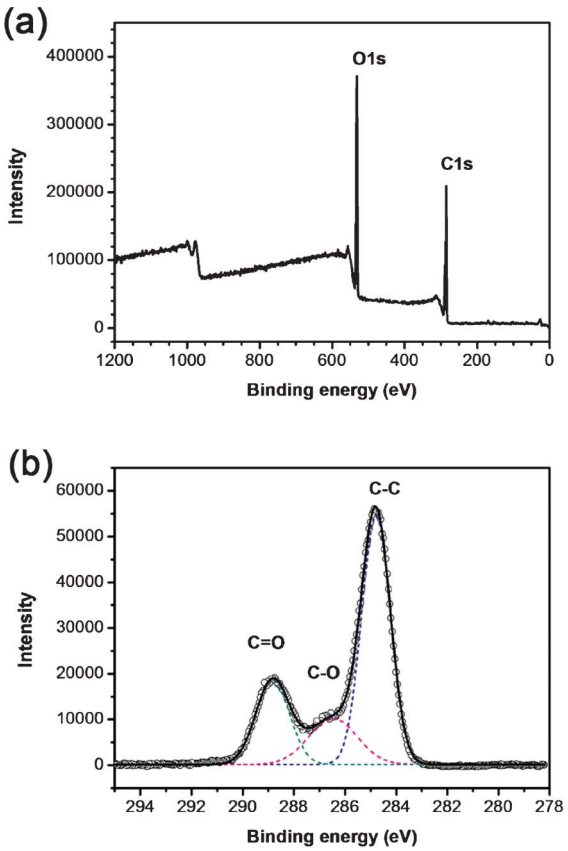

Fig. 2 (a) Survey X-ray photoelectron spectrum of the GCQDs, only C and O signals are detected. (b) C 1s spectrum of the GCQDs. The C1s spectrum has been deconvoluted into three peaks at 284.6, 286.6 and 288.5 eV, corresponding to C–C, C–O and C=O, respectively.

spectrum displays two broad peaks at 1350 and 1598 cm^{-1}, corresponding to D and G bands, respectively. It is well known that the G band is attributed to an E_2g mode of graphite associated with the vibration of sp^2 bonded carbon atoms. The presence of a G band indicates the graphitic character of the GCQDs, in good agreement with the HRTEM image. The I_D/I_G ratio of the GCQDs was measured to be $\sim$1.3, which is similar to that of graphene oxide.[26] The slightly higher D band peak is due to the presence of plenty of oxygen containing groups, considering the fact that the content of carbon not bonded to oxygen is only $\sim$59% (XPS result, Fig. 2).

Similar to other CQDs reported elsewhere, the GCQD solution exhibited strong luminescence. Fig. 4 shows the UV-vis absorption and photoluminescent (PL) emission spectra of the GCQD aqueous solution. It can be clearly observed from the UV-vis spectrum that the GCQDs show absorption in a broad spectrum range. The PL spectrum shows that the sample exhibits a PL emission peak centered at 445 nm, when the excitation wavelength was fixed at 340 nm. Also, it is worth pointing out that the as-prepared GCQDs are very stable in aqueous solution, no obvious aggregation or fluorescence degradation could be observed even after storage at room temperature for several months.

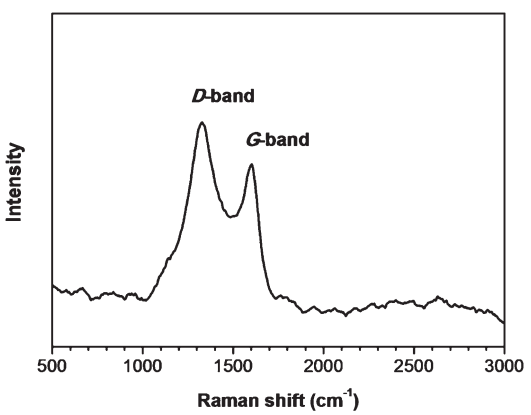

Fig. 3 Raman spectrum of a GCQD sample.

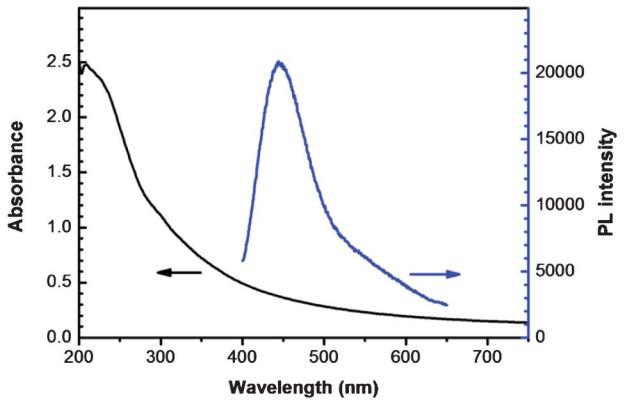

Fig. 4 UV-vis absorption and photoluminescent (PL) emission spectra of an aqueous dispersion of GCQDs.

Typically, the oxygen functional groups on the surfaces of the GCQDs contribute to not only water solubility, but also to their strong interaction with metal ions. For instance, the phenolic hydroxyls would form complexes with Fe^{3+} ions due to coordination. This strong interaction directly provides the possibility of using our GCQDs as a fluorescent probe for Fe^{3+} ion detection. In our experiments, the PL spectra of GCQDs in the presence of different amounts of Fe^{3+} were collected to prove the feasibility of Fe^{3+} detection. As shown in Fig. 5a, the Fe^{3+} can efficiently quench the fluorescence of GCQDs with a detection limit as low as 2 nM, which is much lower than that of carbon nanotubes[27] and graphene nanosheets.[28] With the increase of Fe^{3+} concentration, from 2 nM to 5 μM, the PL intensity gradually decreased to ~20% of its initial value. Fig. 5b shows the dependence of F/F_0 on the concentration of Fe^{3+} ions, where F and F_0 stand for the PL intensities at 445 nm in the presence and absence of Fe^{3+}, respectively. Interestingly, the PL intensity of the GCQDs shows a linear dependence on the Fe^{3+} concentration in the range of 0 to 1 μM, indicating their excellent sensing properties in the detection of trace Fe^{3+}. As iron is an indispensable metal in life forms, for example in metabolism, the detection of Fe^{3+} is of great importance. For example, excess accumulation and deficiency of iron would result in serious health problems related to the kidney and liver, DNA damage, and anemia. Therefore, the highly efficient detection of Fe^{3+} using GCQDs may hold great promise for biochemical analysis, for instance, of iron metabolism, and in anemia diagnosis.

In addition to the high sensitivity for Fe^{3+}, the selectivity of our GCQDs towards different metal ions was also taken into account. Fig. 6a shows the PL spectra of GCQDs in the absence and presence of various metal ions, including Fe^{3+}, Ag^{+}, Cu^{2+}, Ca^{2+}, Zn^{2+}, Co^{2+}, Hg^{2+}, Mg^{2+}, Al^{3+}, Mn^{2+}, Pb^{2+}, Cd^{2+}, Fe^{2+} and Ni^{2+}, respectively, with the same concentration of 1 μM. Notably, the presence of different metal ions would lead to various influences on the PL intensity, however, as compared with other metal ions, Fe^{3+} shows the most obvious quenching effect on the PL intensity (Fig. 6a). Fig. 6b shows the F/F_0 values of GCQDs in the presence of various metal ions, among

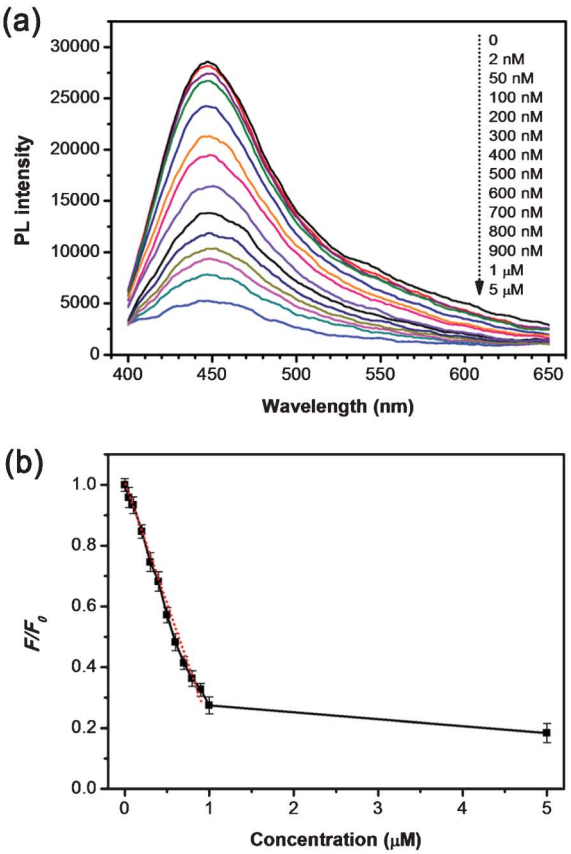

Fig. 5 (a) PL spectra of GCQD aqueous solutions with different Fe^{3+} concentrations (from top to bottom: 0, 2, 50, 100, 200, 300, 400, 500, 600, 700, 800, 900 nM, 1 and 5 μM, respectively). (b) The dependence of F/F_0 on the concentration of Fe^{3+} ions within the range of 0–5 μM. The excitation wavelength was fixed at 340 nm for all the PL spectra. F and F_0 are the PL intensities at 445 nm in the presence and absence of Fe^{3+} ions, respectively.

which Fe^{3+} gives the lowest F/F_0 value of ~0.28, indicting the obvious quenching effect. This result indicates that the GCQDs show high selectivity for Fe^{3+}, and the other metal ions have small influence on the sensing system. The high sensitivity together with the high selectivity for Fe^{3+} make the GCQDs a promising fluorescent sensing platform for the highly efficient detection of Fe^{3+}.

The high selectivity could be attributed to the strong interaction between GCQDs and Fe^{3+}. Shown in Fig. 7 is a schematic illustration of the fluorescence quenching mechanism. It is well known that phenolic hydroxyl groups will form a complex with Fe^{3+}, as shown in the equation in Fig. 7, thus the plentiful phenolic hydroxyl groups on the surfaces of the GCQDs would coordinate with Fe^{3+}. The as-formed Fe-GCQD complexes would facilitate charge transfer and thus restrain exciton recombination, leading to significant fluorescence quenching. As a control experiment, amorphous CQDs were also prepared by microwave treatment of glucose for comparison. As shown in Fig. S3 (ESI†), the PL spectra show negligible change in the presence of Fe^{3+} (1 μM), indicating their incapability for Fe^{3+} detection. These results confirm that the

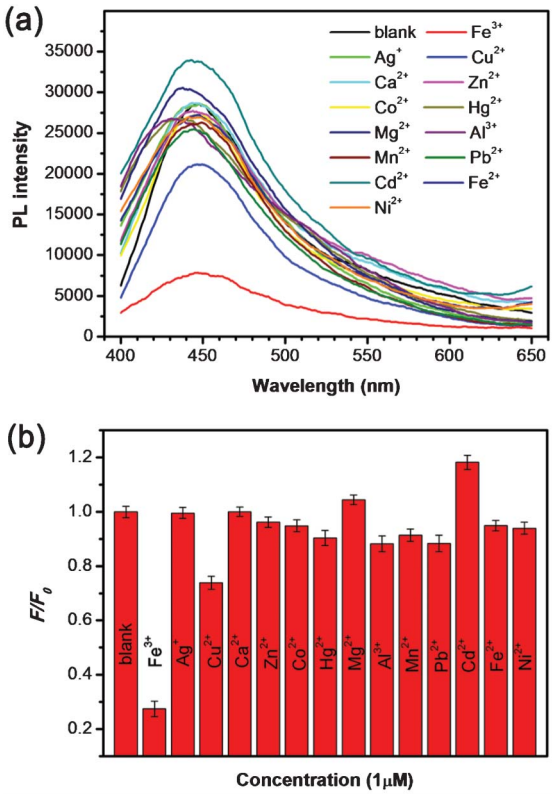

Fig. 6 (a) PL spectra of GCQD aqueous solutions in the presence of different metal ions (the concentrations of the different metal ions are each 1 μM). (b) The different PL intensity ratios (F/F_0) of the GCQD solutions in the presence and absence of various metal ions.

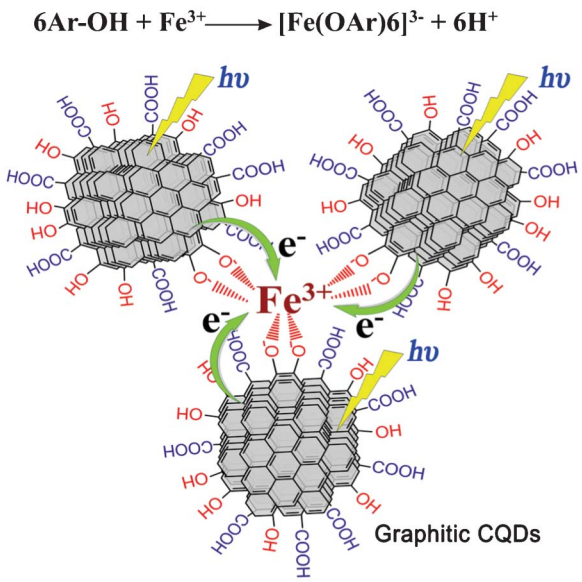

Fig. 7 Schematic illustration of the fluorescence quenching mechanism of the GCQDs in the presence of Fe^{3+}. The top equation shows the formation of a complex between Fe^{3+} and 6 phenolic hydroxyl groups.

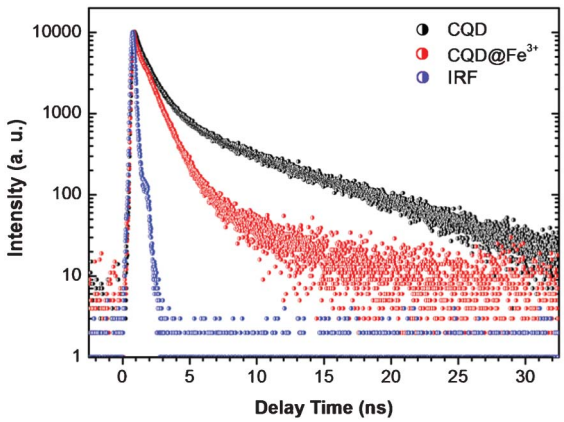

Fig. 8 Fluorescence decay traces of CQDs by TCSPC in the presence (red) and absence (black) of Fe^{3+}. The blue line is the instrument response function.

phenolic hydroxyl groups on the surfaces of the graphitic carbon nanodots are essential for the highly sensitive and selective detection of Fe^{3+}.

To gain further insight into the fluorescence quenching mechanism, time-correlated single-photon counting (TCSPC) experiments were used to test the charge transfer and exciton recombination process of CQDs in the presence and absence of Fe^{3+}. As shown in Fig. 8, the fluorescence lifetime of pure CQDs (black line) is very short, which reflects a fast exciton recombination process. According to the best three-exponential function fitting, there is a very fast decay component (~80%) which is less than the instrument response function (~300 ps), accompanied by two nanosecond components, which are 1 ns (18%) and 7 ns (2%), respectively. After the addition of Fe^{3+} (red line), the ratio of the fast decay component increased, close to ~98%, and the nanosecond components almost disappeared, which are estimated to be 1 ns (~2%) and 5 ns (<1%), respectively. The significantly reduced lifetime indicates a dynamics quenching occurs, and further confirms that there is an ultrafast electron transfer process in the CQD–Fe^{3+} system.

4 Conclusions

In conclusion, carbon nanodots with graphitic crystallinity and surface oxygen-containing groups, denoted as graphitic carbon quantum dots (GCQDs), have been successfully prepared in a green, facile, and scalable manner. By using electrochemical ablation of graphite rod electrodes, water soluble GCQDs with uniform size and high quality could be directly obtained without further purification. The as prepared GCQDs could be used as a fluorescent probe for the highly sensitive and selective detection of Fe^{3+}. The sensing mechanism for the GCQDs could be attributed to the formation of complexes between Fe^{3+} ions and the phenolic hydroxyl groups. Finally, TCSPC experiments have been carried out to test the charge transfer and exciton recombination process of

CQDs in the presence and absence of Fe^{3+}, which confirm a dynamics quenching mechanism.

Acknowledgements

This work is supported by the National Basic Research Program of China (973 Program) (No. 2012CB825800, 2013CB932702), National Natural Science Foundation of China (NSFC) (No. 51132006, 21073127, 21071104), a Foundation for the Author of National Excellent Doctoral Dissertation of China (FANEDD) (No. 200929), a project funded by the Priority Academic Program Development of Jiangsu Higher Education Institutions (PAPD), a Suzhou Planning Project of Science and Technology (ZXG2012028) and a project supported by the Natural Science Foundation of the Jiangsu Higher Education Institutions of China (Grant No. 11KJB150015). We also acknowledge the Hong Kong Scholar Program (XJ2011014).

Notes and references

1 Y. P. Sun, B. Zhou, Y. Lin, W. Wang, K. A. S. Fernando, P. Pathak, M. J. Meziani, B. A. Harruff, X. Wang, H. F. Wang, P. J. G. Luo, H. Yang, M. E. Kose, B. L. Chen, L. M. Veca and S. Y. Xie, *J. Am. Chem. Soc.*, 2006, **128**, 7756–7757.
2 H. T. Li, X. D. He, Z. H. Kang, H. Huang, Y. Liu, J. L. Liu, S. Y. Lian, C. H. A. Tsang, X. B. Yang and S. T. Lee, *Angew. Chem., Int. Ed.*, 2010, **49**, 4430–4434.
3 J. Peng, W. Gao, B. K. Gupta, Z. Liu, R. Romero-Aburto, L. H. Ge, L. Song, L. B. Alemany, X. B. Zhan, G. H. Gao, S. A. Vithayathil, B. A. Kaipparettu, A. A. Marti, T. Hayashi, J. J. Zhu and P. M. Ajayan, *Nano Lett.*, 2012, **12**, 844–849.
4 S. J. Zhuo, M. W. Shao and S. T. Lee, *ACS Nano*, 2012, **6**, 1059–1064.
5 Q. Qu, A. W. Zhu, X. L. Shao, G. Y. Shi and Y. Tian, *Chem. Commun.*, 2012, **48**, 5473–5475.
6 P. Mirtchev, E. J. Henderson, N. Soheilnia, C. M. Yip and G. A. Ozin, *J. Mater. Chem.*, 2012, **22**, 1265–1269.
7 L. Cao, S. T. Yang, X. Wang, P. J. G. Luo, J. H. Liu, S. Sahu, Y. M. Liu and Y. P. Sun, *Theranostics*, 2012, **2**, 295–301.
8 B. S. Harrison and A. Atala, *Biomaterials*, 2007, **28**, 344–353.
9 X. M. Geng, L. Niu, Z. Y. Xing, R. S. Song, G. T. Liu, M. T. Sun, G. S. Cheng, H. J. Zhong, Z. H. Liu, Z. J. Zhang, L. F. Sun, H. X. Xu, L. Lu and L. W. Liu, *Adv. Mater.*, 2010, **22**, 638.
10 H. C. Zhang, H. Huang, H. Ming, H. T. Li, L. L. Zhang, Y. Liu and Z. H. Kang, *J. Mater. Chem.*, 2012, **22**, 10501–10506.
11 H. T. Li, X. D. He, Y. Liu, H. Huang, S. Y. Lian, S. T. Lee and Z. H. Kang, *Carbon*, 2011, **49**, 605–609.
12 H. Zhu, X. L. Wang, Y. L. Li, Z. J. Wang, F. Yang and X. R. Yang, *Chem. Commun.*, 2009, 5118–5120.
13 L. Y. Zheng, Y. W. Chi, Y. Q. Dong, J. P. Lin and B. B. Wang, *J. Am. Chem. Soc.*, 2009, **131**, 4564.
14 Y. Li, Y. Hu, Y. Zhao, G. Shi, L. Deng, Y. Hou and L. Qu, *Adv. Mater.*, 2011, **23**, 776–780.
15 S. N. Baker and G. A. Baker, *Angew. Chem., Int. Ed.*, 2010, **49**, 6726–6744.
16 H. P. Liu, T. Ye and C. D. Mao, *Angew. Chem., Int. Ed.*, 2007, **46**, 6473–6475.
17 X. D. He, H. T. Li, Y. Liu, H. Huang, Z. H. Kang and S. T. Lee, *Colloids Surf., B*, 2011, **87**, 326–332.
18 W. Kwon and S. W. Rhee, *Chem. Commun.*, 2012, **48**, 5256–5258.
19 S. Liu, J. Q. Tian, L. Wang, Y. W. Zhang, X. Y. Qin, Y. L. Luo, A. M. Asiri, A. O. Al-Youbi and X. P. Sun, *Adv. Mater.*, 2012, **24**, 2037–2041.
20 T. W. Sung and Y. L. Lo, *Sens. Actuators, B*, 2012, **165**, 119–125.
21 C. L. Wu and Y. B. Zhao, *Anal. Bioanal. Chem.*, 2007, **388**, 717–722.
22 L. Zhou, Y. H. Lin, Z. Z. Huang, J. S. Ren and X. G. Qu, *Chem. Commun.*, 2012, **48**, 1147–1149.
23 J. M. Liu, L. P. Lin, X. X. Wang, S. Q. Lin, W. L. Cai, L. H. Zhang and Z. Y. Zheng, *Analyst*, 2012, **137**, 2637–2642.
24 Q. Mei, C. Jiang, G. Guan, K. Zhang, B. Liu, R. Liu and Z. Zhang, *Chem. Commun.*, 2012, **48**, 7468–7470.
25 Y. L. Zhang, L. Guo, S. Wei, Y. Y. He, H. Xia, Q. D. Chen, H. B. Sun and F. S. Xiao, *Nano Today*, 2010, **5**, 15–20.
26 L. Guo, R. Q. Shao, Y. L. Zhang, H. B. Jiang, X. B. Li, S. Y. Xie, B. B. Xu, Q. D. Chen, J. F. Song and H. B. Sun, *J. Phys. Chem. C*, 2012, **116**, 3594–3599.
27 L. Jing, C. Liang, X. H. Shi, S. Q. Ye and Y. Z. Xian, *Analyst*, 2012, **137**, 1718–1722.
28 D. Wang, L. Wang, X. Y. Dong, Z. Shi and J. Jin, *Carbon*, 2012, **50**, 2147–2154.

